Published in final edited form as:
Arterioscler Thromb Vasc Biol. 2013 March ; 33(3): 489–500. doi:10.1161/ATVBAHA.112.300893.

Claudin-5 Controls Intercellular Barriers of Human Dermal Microvascular but not Human Umbilical Vein Endothelial Cells

Martin S. Kluger, PhD[1,*], **Paul R. Clark, PhD**[1], **George Tellides, MD, PhD**[2], **Volker Gerke, PhD**[3], and **Jordan S. Pober, MD, PhD**[1]

[1]Department of Immunobiology, Program in Vascular Biology and Therapeutics, Yale University School of Medicine

[2]Department of Surgery, Program in Vascular Biology and Therapeutics, Yale University School of Medicine

[3]Institute of Medical Biochemistry, Center for Molecular Biology of Inflammation, University of Muenster

Abstract

Objective—To assess the role claudin-5, an endothelial cell (EC) tight junction (TJ) protein, plays in establishing basal permeability levels in humans by comparing claudin-5 expression levels in situ and analyzing junctional organization and function in two widely used models of cultured ECs, namely human dermal microvascular (HDM)ECs and human umbilical vein (HUV)ECs.

Methods and Results—By immunofluorescence microscopy, ECs more highly express claudin-5 (but equivalently express VE-cadherin) in human dermal capillaries versus post-capillary venules and in umbilical and coronary arteries versus veins, correlating with known segmental differences in TJ frequencies and permeability barriers. Post-confluent cultured HDMECs express more claudin-5 (but equivalent VE-cadherin) and show higher transendothelial electrical resistance (TEER) and lower macromolecular flux than similarly cultured HUVECs. HDMEC junctions are more complex by transmission electron microscopy and show more continuous claudin-5 immunofluorescence than HUVEC junctions. Calcium chelation or dominant negative VE-cadherin overexpression decreases TEER and disrupts junctions in HUVECs, but not in HDMECs. Claudin-5 overexpression in HUVECs fails to increase TEER or claudin-5 continuity while claudin-5 knockdown in HDMECs, but not HUVECs, reduces TEER and increases antibody accessibility to junctional proteins.

Conclusions—Claudin-5 expression and junctional organization control HDMEC and arteriolar-capillary paracellular barriers whereas HUVEC and venular junctions utilize VE-cadherin.

Keywords

endothelial cell; tight junction; microvessel; permeability; heterogeneity

Microvascular endothelium forms the primary barrier for the bi-directional exchange of blood gases, fluid, soluble nutrients and waste between blood and tissues. Basal microvessel

[*]Corresponding Author: Martin S. Kluger, PhD., 10 Amistad Street, 401A, New Haven, CT 06519 Tel (203) 737-2870, FAX (203) 737-2293. martin.kluger@yale.edu.

Disclosures
None.

permeability varies segmentally being lowest in arterioles, intermediate in continuous capillaries (although very low within the capillaries of the central nervous system; CNS) and greater in post-capillary venules.[1–4] Basal permeability is a function of surface area (vast in capillary beds), flow rate (slowest though capillaries and post capillary venules) and physical properties of the lining endothelium.[5] Routes for molecular exchange across microvascular endothelium can be either paracellular, i.e., between adjacent endothelial cells (ECs) or transcellular via vesicles or vesicular-vacuolar organelles.[6] The principal difference in basal permeability between the capillaries and the post-capillary venules into which they empty is thought to reside in physico-structural properties of EC junctions.[7–9]

Interendothelial junctions may regulate permeability through two different types of cytoskeleton-anchored protein complexes, adherens junctions (AJs) and tight junctions (TJs). Both are composed of transmembrane molecules whose extracellular domains form homophilic attachments that join adjacent ECs. AJs are organized around the transmembrane molecule vascular endothelial (VE-) cadherin and require calcium ions for stability.[10–15] The intracellular portion of VE-cadherin interacts with cytoplasmic proteins (p120, α- and β-catenin, and plakoglobin) that anchor VE-cadherin to the cytoskeleton.[16–21] In epithelial cells, TJ formation but not maintenance requires expression of E-cadherin, the primary cadherin in this cell type.[22] VE-cadherin appears to play a similar role in ECs.[16] In epithelial cells and in ECs, TJs are organized around claudin proteins, the most abundant of which in ECs is claudin-5.[23–25] All claudins are tetramembrane spanning proteins oriented with both their amino and carboxy termini in the cytosol, resulting in the formation of two extracellular loops that control selectivity and adhesion.[26–29] Homophilic claudin-5 interactions at TJs appose adjacent ECs more closely than does VE-cadherin at AJs. Unlike VE-cadherin extracellular adhesion, claudin-5-mediated adhesion is calcium-independent.[30] A conserved carboxy terminus YV-amino acid motif within the intracellular portions of claudins associates with PSD95/Disc Large and Zona occludens (PDZ) domain proteins such as ZO-1 -2, and -3; claudin-5 in particular associates with the multi-PDZ domain protein-1.[31–34] Such interactions that link claudins to the actin cytoskeleton appear in transmission EM as a “diffuse band of dense cytoplasmic material” [35], also referred to as a cytoplasmic plaque.[36–38] In epithelial cells, TJs are spatially segregated into a continuous rim between adjacent cells at the apical-lateral border that is separated from AJs.[35] In contrast, EC TJs do not form a continuous rim and spatially intermix with AJs although it is unclear if TJ and AJ molecules in ECs physically associate.[39] Selective transcellular permeability (permselectivity) in epithelial barriers is mediated by their TJs. TJ abundance in ECs is greatest in arterioles, intermediate in continuous capillaries and least organized in post-capillary venules[7, 8], i.e., TJ frequency generally correlates inversely with the transendothelial permeability properties of EC residing in different types of microvessels. The endothelia of the CNS, which form the highly impermeant blood-brain barrier, is the vascular bed in which TJs are most abundant. These observations suggest that TJs may underlie the segmental gradient of permselectivity observed among peripheral microvascular endothelia. The importance of claudin-5 to EC permselectivity has been demonstrated by the phenotype of claudin-5 knockout mice, which die of cerebral edema shortly after birth, preventing study of claudin-5 in the mature peripheral vasculature.[40] In addition to claudins, TJs may also include other transmembrane proteins such as occludin, junctional adhesion molecules-A,-B or C and, in the case of ECs, endothelial cell selective adhesion molecule; the contributions of these other TJ proteins to transendothelial cell permeability is under investigation, but occludin knockout mice have no obvious vascular phenotype.[41]

Since TJ frequency correlates with microvessel permeability differences in peripheral tissues and since claudin-5 associates with TJs in EC throughout the vascular system, we hypothesized that differences in claudin-5 expression might determine the barrier strength of EC derived from different segments of the human peripheral vasculature, a role described

only in EC derived from brain microvessels. Here we report that differences in claudin-5 expression levels correlate with the barrier strength formed by human ECs *in situ* by an analysis comparing umbilical cord large vessels to skin microvessels. We also report differences in the level of claudin-5 expressed by cultured human dermal microvascular (HDM)ECs that form high resistance barriers vs. cultured human umbilical vein (HUV)ECs that do not. Claudin-5 expression is required to limit paracellular permeability in HDMEC monolayers whereas VE-cadherin performs this function in monolayers of HUVECs. However, claudin-5 overexpression in HUVECs fails to produce high resistance barriers, consistent with our observation that HDMECs and HUVECs organize claudin-5 differently at their respective junctions. These results establish HDMECs as a better model than HUVECs for analysis of human microvascular endothelial TJs.

Methods

For detailed Methods please see Online Supplement

Confocal and epifluorescence immunomicroscopic analyses of human tissues

Specimens of normal human skin, umbilical cord or epicardium were prepared as frozen sections and immunostained using methods and antibodies described in the Online Supplement. For all microscopy procedures, during image acquisition intensity levels were calibrated to the most intense signal and kept constant for a given experiment.

Endothelial cell cultures

HDMECs in normal adult human skin from anonymized donors were isolated as described.[42] Serially passaged HDMECs uniformly express the lymphatic markers Prox-1 and Podoplanin (unpublished data) and concomitantly express E-selectin in response to TNF a characteristic feature of blood vascular ECs.[43] HUVEC cultures were established as previously described[42] then weaned gradually into the same EGM2-MV medium as HDMEC and used between passage 4–6. For all experiments in this study, each EC type seeded onto human plasma fibronectin-coated substrates at approximately 2/3 confluence attained visual confluence at or before 24 h post-plating (designated as Day 0 post-visual confluence).

DNA constructs and transductions

An IL2R-VE retroviral construct was assembled from cDNA of the IL2R-VE-cadherin fusion protein, consisting of the human IL2Rα (CD25) extracellular and transmembrane domains fused to the human VE-cadherin cytoplasmic domain in a pCMV plasmid kindly provided by Dr. Andrew Kowalczyk (Emory University).[44] A human claudin-5 retroviral construct was assembled from human claudin-5 cDNA (clone ID 5242567 obtained from Open Biosystems) and sub-cloned into the retroviral vector pLZRS.CMV. A retroviral EGFP-claudin-5 construct was assembled from cDNA of an N-terminal EGFP-sequence fused to the full length human wild-type cDNA sequence of claudin-5 within the pEGFP-C1-vector (Clontech).[45] Human GIPZ lentiviral shRNAmir constructs used for lentivirus knockdown were obtained as glycerol stabs from Open Biosystems.

FACS analysis and immunoblotting

For FACS analyses of junctional molecule expression, ECs first cultured to day 3 post-visual confluence were immunostained with or without permeabilization. For immunoblot analyses, cultured ECs scrape-harvested on ice into Laemmli buffer were analyzed as described (please see Online Supplement).

Confocal and epifluorescence immunomicroscopic analyses of cells

Immunomicroscopic analyses were performed on ECs on fibronectin-coated glass cover slips at day 3 post-visual confluence unless indicated.

Electron microscopy

ECs were seeded onto fibronectin-coated high-density 0.4 μm pore size 6 well format cell culture inserts (BD Biosciences) and on day 3 post-visual confluence were prepared for EM analysis. Juxtapositions of plasma membrane processes from neighboring EC (overlap regions in Table I) were scored as tongue-in-groove structures where at least one layer has a visible blunt end surrounded on three sides by membrane protrusions originating from an adjacent cell.

Transendothelial flux and TEER measurements

For transendothelial flux measurements, ECs were seeded onto fibronectin-coated 0.4-μm pore 24-well size cell culture inserts (BD Falcon). FITC-dextrans (either 3 kD, or 70 kD, from Invitrogen) suspended in EBM basal medium (base medium for EGM-2MV, Lonza) were added into the apical chamber. Barrier function of ECs cultured on fibronectin-coated 8W10E + gold electrode 8-chamber slides was also assessed by ECIS (Applied BioPhysics).[46]

Calcium chelation assay

The effects of calcium chelation on TEER, intercellular gap formation or displacement of VE-cadherin from EC junctions was assessed by replacing complete medium with warmed serum-free (1% BSA) EBM basal medium; basal medium/BSA supplemented with 4 mM EGTA; basal medium/BSA/EGTA supplemented with 16 mM Ca^{++}; or basal medium/BSA/EGTA supplemented with 16 mM Mg^{++}.

Results

Claudin-5 expression correlates with segmental permeability differences

We first tested the hypothesis that claudin-5 expression by ECs in the peripheral vasculature correlates with known segmental differences in permeability in three human tissues. Umbilical cord is readily available as discarded material and widely used as a source for isolation and culture of human ECs. In the large vessels of the umbilical cord, claudin-5 was expressed at markedly higher levels in arterial ECs than in venous ECs. In contrast, the AJ protein VE-cadherin was more comparably expressed by these same vessel types (Fig. 1A–C). However, since umbilical vessels may differ from other vessel beds with regard to claudin-5 expression due to their exceptional oxygen and pressure levels when carrying blood between placenta and the fetus, we performed additional staining experiments of human adult cardiac vessels. Claudin-5 is expressed at higher levels in human coronary artery than in human coronary vein, whereas in contrast, VE-cadherin is expressed at similar levels in both vessel types. Thus our findings re the relative variability of claudin-5 expression vs. the relative constancy of VE-cadherin expression are not restricted to umbilical vessels (please see Supplemental Fig. I), which also displays immunostained umbilical vessels as confocal microscopy images. In the superficial vascular plexus of human skin, the capillaries are readily distinguished from other microvessels by their unique anatomic position as vascular loops located within the dermal papillae near epidermal rete ridges, whereas the paired arterioles and venules that run parallel to the epidermal surface are located more distal to the rete, and differ by the much greater degree of investment of arterioles compared to venules by SMA-expressing mural cells.[47–50] Within the papillary

dermis, claudin-5 expression was highest in arterioles, intermediate in capillaries and lowest in venules.

Unlike claudin-5, VE-cadherin and in addition the scaffold protein zona-occludens (ZO)-1 were found expressed at largely comparable levels by ECs in all three types of dermal microvessels (Fig. 1D–H and Supplemental Fig. II). These observations are consistent with the hypothesis that claudin-5 expression controls basal paracellular vascular permeability in human peripheral tissues just as it does in the microvessels of the mouse CNS.

Barrier properties, claudin-5 expression and junctional organization of microvascular ECs

We next used ECs cultured from these tissues to study the barrier function of EC junctions. We first quantified the barriers formed by these two cell types using Electrical Cell-substrate Impedance Sensing (ECIS). In EGM2-MV medium, HUVEC monolayers achieved a barrier strength on a fibronectin-coated 8W10E+ electrode array of 1721 +/− 47 ohms and, under identical culture conditions, HDMEC monolayers produce a maximum barrier of 3837 +/− 78 ohms (in eight independent experiments), or a roughly two-fold higher transendothelial electrical resistance (TEER). HUVEC monolayers typically attain maximum barrier integrity soon after HUVEC-HUVEC contacts are initially established as assessed by visual inspection, (designated as day 0 post-visual confluence). In contrast, HDMECs form a barrier of comparable strength to that of HUVECs at visual confluence, but then further increase their barrier over the next three-five days before reaching a plateau at the higher level of TEER described above (Fig. 2A). The TEER time courses and maximal TEER levels of both EC cell types were similar whether the electrodes were coated with human fibronectin or with human collagen IV (please see Supplemental Fig. III) and all subsequent studies in this report used fibronectin-coated surfaces. Consistent with a higher level of TEER, HDMEC monolayers limited transendothelial flux of 3000 or 70,000 D FITC-dextrans compared to HUVECs (Fig. 2B). We also examined if HDMEC limit transendothelial flux via a more effective paracellular barrier or via slower vesicular transport by comparing transendothelial flux at 37° C, a temperature that permits endocytosis, and at 4° C, a temperature that does not. These measurements showed that differences in flux of 3 kDa FITC-dextran across HDMEC and HUVEC monolayers were similar at both temperatures through 6 hours, when the concentration gradient between the upper and lower transwells still remained far from equilibrium (please see Supplemental Fig IV), strongly suggesting that the difference among EC types is due to differences in their paracellular barriers and independent of vesicular transport.

To further analyze the intercellular junctions that formed in culture, we examined post-confluent monolayers of HDMECs and HUVECs by transmission EM. In microscope fields displaying regions of overlap by adjacent ECs, HDMECs formed multi-layered protrusions that interdigitated in a tongue-in-groove fashion, creating a labyrinth-like paracellular path (Fig. 2C, top). In contrast, HUVEC junctions have more simple topologies of adjacent cells that simply overlap (Fig. 2D, top). Tongue-in-groove structures in overlap regions of HDMECs are six-fold greater than in HUVEC monolayers, correlating with increased barrier formation by HDMECs (please see Table I). In both EC types we observed membrane approximations that appeared as “kissing points” near diffuse cytoplasmic densities, structures generally interpreted as TJs. Such TJ structures were significantly more numerous at HDMEC than HUVEC junctions and their number correlated with TEER measured on the same EC lines. These differences in the morphology of intercellular junctions likely underlie the observed differences in EC barrier properties.

To explore molecular differences at EC junctions, we compared the expression levels of claudin-5 and other EC junctional proteins between these two cultured EC types by FACS analysis and immunoblotting. On day 3 post-visual confluence, HDMECs uniformly express

claudin-5 at levels more than twice high as HUVECs but express VE-cadherin (CD144) and ZO-1 at levels comparable to HUVECs as quantified by FACS (Fig. 3A). Also by densitometric analysis of immunoblotting, claudin-5 expression on day 3 post-visual confluence is two-fold greater in HDMECs than in HUVECs and VE-cadherin is expressed at equivalent levels in both EC types (Fig. 3B and C; normalized to β-actin). Occludin was more abundant in HUVEC and barely detectable in HDMEC. Interestingly, during three days at post-confluence claudin-5 increased 3.6-fold in HDMEC ($P<0.5$), but VE-cadherin did not. Increases in claudin-5 expression levels correlate with the TEER increase noted for HDMEC monolayers, but despite considerable HUVEC expression of claudin-5 by day 3 post-confluence, HUVEC monolayers showed no increase in TEER (Fig. 3C). By immunoblotting, ZO-1 expression did not change at post-confluence in both EC types (please see Supplemental Fig V).

We next used confocal fluorescence immunomicroscopy to characterize spatial patterns of claudin-5 and VE-cadherin expression at HDMEC and HUVEC junctions. In HDMECs on day 0 post-visual confluence, claudin-5 localization at junctions is minimal, but both the junctional localization and intensity of claudin-5 staining progressively increase, condensing by day 3 post-confluence to a thin but bright continuous band outlining the cell (Fig. 4A). However in HUVECs, the staining pattern of claudin-5 remains sawtooth and discontinuous at many points along their borders through day 3 post-visual confluence (Fig. 4B), never producing the continuous pattern of junctional staining characteristic of HDMECs. Localization of VE-cadherin to the cell junction, as detected with a goat antibody to an intracellular epitope in permeabilized cells, preceded the junctional localization of claudin-5 in both EC types (Fig. 4A). However, in HDMECs that were not permeabilized, staining of VE-cadherin with antibody to an extracellular epitope[13] decreased as the cells progressively tightened their barrier, suggesting reduced antibody access to the intercellular space (Fig. 4C). This reduced staining of extracellular VE-cadherin epitopes was not observed in post-confluent HUVECs (Fig. 4D) and similar changes in accessibility to extracellular epitopes of PECAM-1 were seen in post-confluent HDMECs but not HUVECs (data not shown). Thus a progressive change in claudin-5 organization as well as expression at the intercellular junctions of HDMEC monolayers correlates with both an increase in TEER and a reduction in accessibility to the paracellular space.

Cadherins are necessary for formation of TJs but may not be necessary for their maintenance. Therefore, we tested the role of VE-cadherin in established HDMEC and HUVEC monolayers by overexpression of a dominant negative fusion protein in which the VE-cadherin intracellular cytoplasmic domain is fused to the extracellular and transmembrane domains of interleukin-2 receptor α chain (CD25).[44] The VE-cadherin intracellular domain of this construct (IL2R-VE) displaces endogenous VE-cadherin from the junction and increases permeability in immortalized HMEC-1 cell monolayers.[17, 44] We confirmed by immunoblotting, first with an anti-IL2Rα antibody (that only recognizes expression of IL2R-VE) and then with goat polyclonal anti-VE-cadherin (which recognizes both IL2R-VE and endogenous VE-cadherin) that IL2R-VE was expressed at the expected size and at comparable levels in both FACSorted EC lines (Fig. 5A and B). Both HDMECs and HUVECs overexpressing this construct down regulate surface expression of endogenous VE-cadherin without affecting levels of claudin-5 expression as assessed by FACS analysis (ref. 21 and unpublished data). IL2R-VE overexpression decreased TEER by 60% in HUVEC monolayers, but in post-confluent HDMEC monolayers merely delayed reaching the maximal level of TEER, which was unchanged (Fig. 5C). Consistent with the effect of dominant negative VE-cadherin overexpression on TEER, the junctions of transduced HUVECs but not HDMECs were disrupted and formed gaps (Fig. 5D). We also exploited the fact that VE-cadherin based AJ adhesion is strongly calcium-dependent whereas with claudin-based TJ adhesion is not[11, 30] by replacing EGM2-MV medium on EC monolayers

grown on ECIS electrodes with serum- and growth factor-free basal medium containing 4 mM EGTA (a two-fold molar excess over medium [Ca^{++}]). Within seconds after calcium chelation, HUVEC TEER fell by 75% while HDMEC TEER persisted at normal levels through one hour after which their barriers gradually weaken (Supplemental Fig. VI and data not shown). The fall in TEER correlated with the development of visible gaps between adjacent HUVECs, a finding not observed in HDMEC monolayers subjected to calcium chelation. VE-cadherin in HUVECs, but not in HDMECs, was displaced from intercellular junctions by EGTA-containing basal medium as judged by epifluorescence immunomicroscopy. Overall, these observations suggest that post-confluent HDMEC junctions are far less dependent than HUVEC on VE-cadherin for their integrity and function.

Claudin-5 is required for HMDEC, not HUVEC barrier properties

To further contrast the role of claudin-5 in HUVECs, we transduced these cells with a drug selectable retrovirus encoding N-terminally tagged EGFP-claudin-5 (EGFP-claudin-5) or EGFP alone (negative control). Following selection, HUVECs strongly expressed EGFP-claudin-5 or EGFP (control) by FACS analysis. Immunoblotting confirmed HUVEC expression of EGFP-claudin-5 protein at the expected apparent molecular weight relative to endogenous claudin-5. Despite EGFP-claudin-5 overexpression at HDMEC-like levels, fluorescence in HUVECs localized to junctions only in the discontinuous, sawtooth pattern characteristic of endogenous claudin-5 in this EC type. Although many junctions in HDMECs overexpressing EGFP-claudin-5 also showed a disrupted fluorescence pattern, some junctions in post-confluent monolayers of transduced HDMEC monolayers showed patterns of EGFP fluorescence that was continuous, similar to the pattern of immunostaining of endogenous claudin-5 in this cell type (please see Supplemental Fig. VII). Free EGFP did not localize to junctions in either cell type but unexpectedly reduced the level of TEER. We therefore compared the functional effects of overexpressing untagged claudin-5 vs. a control retroviral vector minus an insert. Claudin-5 overexpression in HUVECs was confirmed by immunoblotting and by increased immunostaining staining at junctions that, like EGFP-claudin-5, displayed patterns that were discontinuous and sawtooth. Overexpression of claudin-5 to levels seen in HDMECs did not increase TEER in post-visual confluent HUVECs, but did inhibit gap formation between cells in response to chelation of calcium (please see Supplemental Fig. VIII; the intercellular space after EGTA treatment corrected for medium control in μm^2 +/− SEM was 2610 +/− 163 for claudin-5-transduced HUVEC versus 7718 +/− 685 for control–transduced HUVEC, a statistically significant difference *P = 0.002 by a two-tailed t-test). Thus increased claudin-5 expression is insufficient to form high resistance paracellular junctions in HUVECs, probably because HUVECs fail to organize claudin-5 in the manner observed in HDMECs.

We next tested if endogenous claudin-5 expression is necessary for barrier functions in ECs by means of lentivirus-mediated shRNA knockdown. Two different lentiviral shRNA constructs targeting claudin-5 mRNA effectively reduced claudin-5 protein expression in HUVECs and HDMECs without affecting protein expression of VE-cadherin (Fig. 6A). The extent of claudin-5 knockdown correlated with TEER decreases in HDMEC, and with the most effective shRNA vector HDMEC TEER attained only one-half that of control transduced HDMECs on day 4 post-confluence (Fig. 6B). Claudin-5 shRNA knockdown also restored access to intercellular junctions between post-confluent HDMECs, allowing for bright staining of extracellular epitopes of VE-cadherin (Fig. 6C) or of PECAM-1 (data not shown). In contrast, claudin-5 knockdown had no measurable effect on TEER levels in HUVECs (Fig. 6B). ShRNA knockdown of the tight junction protein, occludin, which gradually localizes to junctions and appears to increase expression from day 0 to day 3 post-confluence in HUVECs, did not affect HUVEC TEER (please see Supplemental Fig. IX).

Thus claudin-5 expression in HDMECs appears essential for the characteristics that distinguish HDMEC junctions from those of HUVECs but plays no apparent role in HUVEC junctions.

Discussion

In our study, *in situ* expression of claudin-5 in human vascular EC, the signature protein component of endothelial TJs, correlates both with historically established variations of vascular EC barrier function to blood molecules[1–4] and with the presence of TJs observed by EM[7–9] being higher in umbilical artery than vein and higher in arterioles and the continuous capillaries than in the venules of the dermal superficial vascular plexus. This suggested the simple hypothesis that variations in claudin-5 expression would correlate with TJ formation and with less permeable barriers in cultured human ECs from these same tissues. Indeed, we found that cultured HDMECs express claudin-5 at higher levels and form monolayers with reduced macromolecular flux and approximately two-fold higher levels of TEER than do cultured HUVECs. We directly tested the importance of claudin-5 in HDMECs by shRNA knockdown, which resulted in reduced TEER and increased access of antibodies to the intercellular junctions. Furthermore, the barrier function of post-confluent HDMECs, but not of HUVECs, attained a state after several days that appeared independent of VE-cadherin as shown by the limiting effects on TEER and gap formation of both calcium chelation and overexpression of a dominant negative form of VE-cadherin. Moreover, as the HDMEC barrier progressively increased at post-confluence, there was a parallel increase in HDMEC expression of claudin-5. However, claudin-5 expression also increased in post-confluent HUVECs and these cultures failed to increase their barrier to electrical current. TEER in HUVEC cultures was also unaffected by either knockdown or by overexpression of claudin-5, although HUVEC that overexpressed claudin-5 did acquire a HDMEC-like resistance to intercellular gap formation induced by chelation of calcium. We attribute the difference in barrier formation between HDMECs and HUVECs to the manner in which endogenous or overexpressed claudin-5 is organized by these two cell types. Specifically, claudin-5 in HDMECs coalesced over time into a continuous and intensely focused staining at regions of HDMEC intercellular contact that is distinctly different from the sawtooth, discontinuous distribution of claudin-5 at the contact points formed by adjacent HUVECs. Junctions also appear more complex in HDMEC than HUVEC monolayers by transmission EM. Specifically, in HDMECs we observed higher density of TJs identified as kissing points and more frequent interdigitating membrane tongue-in-groove morphologies than in HUVECs. Such interdigitating junctions have been observed *in vivo* [51] and correlate with the impermeability to Evans Blue dye.[52] These data demonstrate that phenotypic differences in the intercellular junctions among human EC types that correlate with permeability are represented in cultured HDMECs and HUVECs.

The term “junctional maturation” has been used to describe time-dependent re-organization in the barriers that form in epithelial cells[53, 54] and a similar process has been observed to occur in the CNS and in brain-derived ECs *in vitro*.[55, 56] Our data suggest that cultured HDMECs undergo a claudin-5-dependent tight junction maturation, contributing both to the progressive rise in TEER and to the progressive exclusion of antibodies from the interjunctional space. Although HDMECs continue to divide, increasing cell numbers at post-confluence, this change is insufficient to account for the observed maturation of their junctions as HUVEC similarly divide and increase in cell number without showing junctional maturation. Futhermore, the junctional maturation of HDMECs must depend on more than simply transporting claudin-5 to plasma membrane regions because both HDMECs and HUVECs localize claudin-5 to regions of EC-EC membrane contact. The failure of claudin-5 to influence the barrier formed by cultured HUVECs suggests that EC proteins other than claudin-5 must also contribute to barrier formation, perhaps by

organizing claudin-5 into the structures we observe as tight, continuous bands in cultured HDMECs. Junction maturation requires coordinated expression, localization and interaction of transmembrane proteins such as VE-cadherin or claudin-5 with linker molecules, cytoskeleton adaptor molecules and interactive enzymes that gradually assemble into a cytoplasmic plaque that anchors an AJ or TJ complex to the actin cytoskeleton.[19, 34, 38, 57, 58] Proteins that help link claudins to the EC cytoskeleton include ZO-1, -2 or -3 and as described for claudin-5, multi-PDZ domain protein-1.[31–33] Alternatively, HDMECs and HUVECs may differentially express other transmembrane TJ proteins that aid or inhibit cytoplasmic plaque assembly, respectively. For example, occludin, which is expressed at higher levels in HUVECs than HDMECs, could potentially interfere with claudin-5 organization, perhaps by competing for the same interacting partner. However, occludin knockdown in HUVECs did not cause an increase in TEER, arguing against this interpretation (please see Supplemental Fig. IX). Consistent with our observations that claudin-5-dependent barriers vary by EC type, others have observed claudin-5 overexpression leads to no increase[59] or only a modest enhancement[60] of barrier function by overexpression of claudin-5 in HUVECs. The modest enhancement of claudin-5 expression increase in HUVEC driven by lentivirus overexpression (described as "massive")[60] was likely greater than the amount of retrovirus-driven claudin-5 overexpression in our study. In contrast to the findings reported by Yuan et al.,[59] we found no effect of RNAi-mediated knock down of claudin-5 in HUVECs; the reason for this discrepancy is unclear, but we have found that transfection conditions used to introduce siRNA can affect barriers in a manner not seen with lentivirus transduction of shRNA. HUVEC barriers in our study and those of others appear mainly dependent on VE-cadherin at AJs.[17] The barrier properties of HMEC-1, an immortalized EC line derived from human dermal foreskin that is often used as a model for microvascular EC[61] also differs from the HDMECs we have studied in that the HMEC-1 barrier is, like HUVECs, VE-cadherin-dependent.[44] Therefore HDMECs may be more useful than HMEC-1s for studying capillary barriers. HDMEC overexpressing IL2R-VE cultured overnight to 80% confluence were reported to form gaps.[21] Our observations differ from this report, probably because we studied post-confluent monolayers in which junctions had matured. Our data are unexpected in that Capaldo et al.[22] is the only prior report in the epithelial cell literature of which we are aware demonstrating that cadherins are not necessary to maintain cell junctions, in contrast to a very large number of papers that claim the opposite. Our data do not show that HDMEC barriers are completely VE-cadherin independent, but are unequivocal that barriers formed by HDMEC are far less dependent on VE-cadherin than those of HUVEC.

Despite a common embryological origin and a shared number of features that lead to defining ECs as a distinct cell type, ECs adapt their morphological and functional features at distinct anatomic sites and among different vascular segments of the same tissue.[62] HUVECs were the first and remain the most widely used model system to study ECs in culture. But as others have shown and we confirm here, junctional barriers in these cells are largely maintained by VE-cadherin-organized AJs, rather than claudin-organized TJs. They are a useful model for TJ-poor post-capillary venules,[13, 17, 63] but not for TJ-rich capillaries. At present there is no comparably well-accepted *in vitro* model for studying the distinct features of continuous capillaries, possibly since microvascular ECs show greater tissue to tissue variation than do systemic large vessel ECs. Several investigators have concentrated on brain-derived ECs because they wish to study the unique properties of the blood-brain barrier. However, human material for primary cultures is limiting, provides variable or unstable phenotypes, and many such studies rely on immortalized cell lines.[64, 65] Furthermore, the formation of a CNS-like tight barriers by such cells often requires CNS-derived extrinsic factors like astrocyte-conditioned medium.[66, 67] The unique properties of the vasculature within the CNS also raises questions about whether findings using these cells can be extrapolated to peripheral microvessels. We have chosen to study HDMECs because

we can readily compare findings made with this cell type in culture with cells in an accessible tissue, namely human skin. There are complications in this choice. Cultured HDMECs derive from a mixture of EC types originating in lymphatic microvessels as well as from microvessels of the blood circulatory system. Our cultured HDMECs uniformly express lymphatic markers Prox-1 and podoplanin, but also behave like blood vessel ECs by uniformly expressing E-selectin in response to tumor necrosis factor or interleukin-1 (ref. 43 and unpublished data, MSK and JSP). Despite their heterogeneous origin, FACS analyses of our HDMECs in Fig. 3 reveal a tight, uniform expression of the junctional molecules claudin-5, VE-cadherin and ZO-1. Moreover, lymphatic vessels form barriers dependent on expression of the same TJ molecules as blood vessels.[68, 69] With regard to intercellular junctions, both EC types form similar structures at the level of transmission electron microscopy.[70] In contrast to HDMEC used in our studies, Prox-1-negative dermal blood microvessel-derived EC (BEC purchased from Lonza) show decreased contact inhibition of migration so that confluent cells crawl over each other and form unstable intercellular barriers such that TEER decreases over time at confluence when cultured on human fibronectin or on collagen IV (MSK, unpublished observations). Such cells are thus less useful for the study of EC intercellular barriers. The decision of which EC culture model is best to study should rest on whether a distinct EC phenotype observed *in situ* is preserved *in vitro*, such as AJs in cultured HUVECs or TJs in cultured HDMECs. For example, to investigate the capillary leak syndrome associated with multi-organ failure in sepsis, HDMECs, which more faithfully represent the barrier properties of capillaries, would be a better model than HUVECs, which more closely resemble post-capillary venules.

It would be tempting to speculate that the sawtooth patterns we observed by immunofluorescence at HUVEC junctions for claudin-5 but not VE-cadherin may reflect differences in junctional ultrastructure observed by EM in which HUVEC junctions appeared to overlap and showed far fewer of the tongue-in-groove interdigitations than did HDMEC. In HDMEC, membrane interdigitations may provide a topology favoring the fine, continuous claudin-5 patterns we observed by confocal and epi-fluorescence microscopy, while in HUVEC, the simple overlapping of membranes from neighboring cells may distribute claudin-5 more spaciously, potentially explaining why relatively fewer tight junctions were counted per region of overlapping membranes in this EC type. However, in Figure 4, HUVECs seem no less adept than HDMECs at forming VE-cadherin-based adherens junctions, which by virtue of the long VE-cadherin extracellular region consisting of five contiguous IgG domains, may facilitate HUVEC-HUVEC interaction despite the absence of tongue-in-groove interdigitations.

In conclusion, our data show that (1) claudin-5 is expressed differentially and in a manner correlating with known TJ frequencies and barrier strengths of human blood vessels from outside of the CNS, suggesting that claudin-5 could contribute to the segmentally arranged barrier heterogeneity of peripheral endothelium; (2) claudin-5 expression is necessary but insufficient for establishing paracellular barriers in cultured EC; and (3) claudin-5 expression, when continuously organized at tight junctions of post-confluent monolayers of HDMEC but not HUVEC, is critical for the maintenance of paracellular barriers *in vitro* independently of VE-cadherin.

Supplementary Material

Refer to Web version on PubMed Central for supplementary material.

Acknowledgments

We thank Lisa Gras, Louise Benson and Dr. Yirong Kong for technical assistance.

Sources of Funding

Supported by NIH grant R01-HL036003 to MSK and JSP.

References

1. Rous P, Gilding HP, Smith F. The gradient of vascular permeability. J Exp Med. 1930; 51:807–830. [PubMed: 19869729]
2. Rous P, Smith F. The gradient of vascular permeability:III. The gradient along the capillaries and venules of frog skin. J Exp Med. 1931; 53:219–242. [PubMed: 19869837]
3. Smith F, Rous P. The gradient of vascular permeability:IV. The permeability of the cutaneous venules and its functional significance. J Exp Med. 1931; 54:499–514. [PubMed: 19869936]
4. Smith F, Rous P. The gradient of vascular permeability:II. The conditions in frog and chicken muscle, and in the mammalian diaphragm. J Exp Med. 1931; 53:195–217. [PubMed: 19869836]
5. Duran, WN.; Sanchez, FA.; Breslin, JW. Microcirculatory exchange function. In: Tuma, RF.; Duran, WN.; Ley, K., editors. Handbook of physiology: Microcirculation. New York: Elsevier-Academic Press; 2008. p. 81-124.
6. Komarova Y, Malik AB. Regulation of endothelial permeability via paracellular and transcellular transport pathways. Annu Rev Physiol. 2010; 72:463–493. [PubMed: 20148685]
7. Simionescu M, Simionescu N, Palade GE. Segmental differentiations of cell junctions in the vascular endothelium. The microvasculature. J Cell Biol. 1975; 67:863–885. [PubMed: 1202025]
8. Simionescu N, Simionescu M, Palade GE. Structural basis of permeability in sequential segments of the microvasculature of the diaphragm.II. Pathways followed by microperoxidase across the endothelium. Microvasc Res. 1978; 15:17–36. [PubMed: 634154]
9. Schneeberger EE. Segmental differentiation of endothelial intercellular junctions in intra-acinar arteries and veins of the rat lung. Circ Res. 1981; 49:1102–1111. [PubMed: 7296777]
10. Ali J, Liao F, Martens E, Muller WA. Vascular endothelial cadherin (VE-cadherin): Cloning and role in endothelial cell-cell adhesion. Microcirculation. 1997; 4:267–277. [PubMed: 9219219]
11. Breviario F, Caveda L, Corada M, Martin-Padura I, Navarro P, Golay J, Introna M, Gulino D, Lampugnani MG, Dejana E. Functional properties of human vascular endothelial cadherin (7b4/cadherin-5), an endothelium-specific cadherin. Arterioscler Thromb Vasc Biol. 1995; 15:1229–1239. [PubMed: 7627717]
12. Corada M, Mariotti M, Thurston G, Smith K, Kunkel R, Brockhaus M, Lampugnani MG, Martin-Padura I, Stoppacciaro A, Ruco L, McDonald DM, Ward PA, Dejana E. Vascular endothelial-cadherin is an important determinant of microvascular integrity in vivo. Proc Natl Acad Sci U S A. 1999; 96:9815–9820. [PubMed: 10449777]
13. Corada M, Liao F, Lindgren M, Lampugnani MG, Breviario F, Frank R, Muller WA, Hicklin DJ, Bohlen P, Dejana E. Monoclonal antibodies directed to different regions of vascular endothelial cadherin extracellular domain affect adhesion and clustering of the protein and modulate endothelial permeability. Blood. 2001; 97:1679–1684. [PubMed: 11238107]
14. Nagafuchi A, Shirayoshi Y, Okazaki K, Yasuda K, Takeichi M. Transformation of cell adhesion properties by exogenously introduced E-Cadherin cDNA. Nature. 1987; 329:341–343. [PubMed: 3498123]
15. Schulte D, Kuppers V, Dartsch N, Broermann A, Li H, Zarbock A, Kamenyeva O, Kiefer F, Khandoga A, Massberg S, Vestweber D. Stabilizing the VE-cadherin-catenin complex blocks leukocyte extravasation and vascular permeability. EMBO J. 2011; 30:4157–4170. [PubMed: 21857650]
16. Dejana E, Tournier-Lasserve E, Weinstein BM. The control of vascular integrity by endothelial cell junctions: Molecular basis and pathological implications. Dev Cell. 2009; 16:209–221. [PubMed: 19217423]
17. Guo M, Wu MH, Granger HJ, Yuan SY. Transference of recombinant VE-cadherin cytoplasmic domain alters endothelial junctional integrity and porcine microvascular permeability. J Physiol. 2004; 554:78–88. [PubMed: 14678493]
18. Lampugnani MG, Corada M, CaVEda L, Breviario F, Ayalon O, Geiger B, Dejana E. The molecular organization of endothelial cell to cell junctions: Differential association of plakoglobin,

beta-catenin, and alpha-catenin with vascular endothelial cadherin (VE-cadherin). J Cell Biol. 1995; 129:203–217. [PubMed: 7698986]

19. Navarro P, Caveda L, Breviario F, Mandoteanu I, Lampugnani MG, Dejana E. Catenin-dependent and -independent functions of vascular endothelial cadherin. J Biol Chem. 1995; 270:30965–30972. [PubMed: 8537353]
20. Vestweber D, Broermann A, Schulte D. Control of endothelial barrier function by regulating vascular endothelial-cadherin. Curr Opin Hematol. 2010; 17:230–236. [PubMed: 20393283]
21. Xiao K, Allison DF, Buckley KM, Kottke MD, Vincent PA, Faundez V, Kowalczyk AP. Cellular levels of p120 catenin function as a set point for cadherin expression levels in microvascular endothelial cells. J Cell Biol. 2003; 163:535–545. [PubMed: 14610056]
22. Capaldo CT, Macara IG. Depletion of E-cadherin disrupts establishment but not maintenance of cell junctions in Madin-Darby canine kidney epithelial cells. Mol Biol Cell. 2007; 18:189–200. [PubMed: 17093058]
23. Morita K, Sasaki H, Furuse M, Tsukita S. Endothelial claudin: claudin-5/TMVCF constitutes tight junction strands in endothelial cells. J Cell Biol. 1999; 147:185–194. [PubMed: 10508865]
24. Morita K, Sasaki H, Furuse K, Furuse M, Tsukita S, Miyachi Y. Expression of claudin-5 in dermal vascular endothelia. Exp Dermatol. 2003; 12:289–295. [PubMed: 12823443]
25. Anderson JM, Van Itallie CM. Physiology and function of the tight junction. Cold Spring Harb Perspect Biol. 2009; 1:a002584. [PubMed: 20066090]
26. Furuse M, Sasaki H, Tsukita S. Manner of interaction of heterogeneous claudin species within and between tight junction strands. J Cell Biol. 1999; 147:891–903. [PubMed: 10562289]
27. Piontek J, Winkler L, Wolburg H, Muller SL, Zuleger N, Piehl C, Wiesner B, Krause G, Blasig IE. Formation of tight junction: Determinants of homophilic interaction between classic claudins. FASEB J. 2008; 22:146–158. [PubMed: 17761522]
28. Piehl C, Piontek J, Cording J, Wolburg H, Blasig IE. Participation of the second extracellular loop of claudin-5 in paracellular tightening against ions, small and large molecules. Cell Mol Life Sci. 2010; 67:2131–2140. [PubMed: 20333434]
29. Piontek J, Fritzsche S, Cording J, Richter S, Hartwig J, Walter M, Yu D, Turner JR, Gehring C, Rahn HP, Wolburg H, Blasig IE. Elucidating the principles of the molecular organization of heteropolymeric tight junction strands. Cell Mol Life Sci. 2011; 68:3903–3918. [PubMed: 21533891]
30. Kubota K, Furuse M, Sasaki H, Sonoda N, Fujita K, Nagafuchi A, Tsukita S. Ca(2+)-independent cell-adhesion activity of claudins, a family of integral membrane proteins localized at tight junctions. Curr Biol. 1999; 9:1035–1038. [PubMed: 10508613]
31. Itoh M, Furuse M, Morita K, Kubota K, Saitou M, Tsukita S. Direct binding of three tight junction-associated MAGUKs, ZO-1, ZO-2, and ZO-3, with the COOH termini of claudins. J Cell Biol. 1999; 147:1351–1363. [PubMed: 10601346]
32. Jeansonne B, Lu Q, Goodenough DA, Chen YH. Claudin-8 interacts with multi-PDZ domain protein 1 (MUPP1) and reduces paracellular conductance in epithelial cells. Cell Mol Biol (Noisy-le-grand). 2003; 49:13–21. [PubMed: 12839333]
33. Poliak S, Matlis S, Ullmer C, Scherer SS, Peles E. Distinct claudins and associated PDZ proteins form different autotypic tight junctions in myelinating schwann cells. J Cell Biol. 2002; 159:361–372. [PubMed: 12403818]
34. Wittchen ES, Haskins J, Stevenson BR. Protein interactions at the tight junction. Actin has multiple binding partners, and ZO-1 forms independent complexes with ZO-2 and ZO-3. J Biol Chem. 1999; 274:35179–35185. [PubMed: 10575001]
35. Farquhar MG, Palade GE. Junctional complexes in various epithelia. J Cell Biol. 1963; 17:375–412. [PubMed: 13944428]
36. Fanning AS, Ma TY, Anderson JM. Isolation and functional characterization of the actin binding region in the tight junction protein ZO-1. FASEB J. 2002; 16:1835–1837. [PubMed: 12354695]
37. Furuse M. Molecular basis of the core structure of tight junctions. Cold Spring Harb Perspect Biol. 2010; 2:a002907. [PubMed: 20182608]

38. Guillemot L, Paschoud S, Pulimeno P, Foglia A, Citi S. The cytoplasmic plaque of tight junctions: A scaffolding and signalling center. Biochimica et Biophysica Acta (BBA) -Biomembranes. 2008; 1778:601–613.
39. Ruffer C, Strey A, Janning A, Kim KS, Gerke V. Cell-cell junctions of dermal microvascular endothelial cells contain tight and adherens junction proteins in spatial proximity. Biochemistry. 2004; 43:5360–5369. [PubMed: 15122902]
40. Nitta T, Hata M, Gotoh S, Seo Y, Sasaki H, Hashimoto N, Furuse M, Tsukita S. Size-selective loosening of the blood-brain barrier in claudin-5-deficient mice. J Cell Biol. 2003; 161:653–660. [PubMed: 12743111]
41. Saitou M, Furuse M, Sasaki H, Schulzke JD, Fromm M, Takano H, Noda T, Tsukita S. Complex phenotype of mice lacking occludin, a component of tight junction strands. Mol Biol Cell. 2000; 11:4131– 4142. [PubMed: 11102513]
42. Kluger MS, Johnson DR, Pober JS. Mechanism of sustained E-selectin expression in cultured human dermal microvascular endothelial cells. J Immunol. 1997; 158:887–896. [PubMed: 8993008]
43. Kluger MS, Shiao SL, Bothwell AL, Pober JS. Cutting edge: Internalization of transduced E-selectin by cultured human endothelial cells: Comparison of dermal microvascular and umbilical vein cells and identification of a phosphoserine-type di-leucine motif. J Immunol. 2002; 168:2091–2095. [PubMed: 11859093]
44. Venkiteswaran K, Xiao K, Summers S, Calkins CC, Vincent PA, Pumiglia K, Kowalczyk AP. Regulation of endothelial barrier function and growth by VE-cadherin, plakoglobin, and beta-catenin. Am J Physiol Cell Physiol. 2002; 283:C811–821. [PubMed: 12176738]
45. Ruffer C, Gerke V. The C-terminal cytoplasmic tail of claudins 1 and 5 but not its PDZ-binding motif is required for apical localization at epithelial and endothelial tight junctions. Eur J Cell Biol. 2004; 83:135–144. [PubMed: 15260435]
46. Giaever I, Keese CR. Micromotion of mammalian cells measured electrically. Proc Natl Acad Sci U S A. 1991; 88:7896–7900. [PubMed: 1881923]
47. Yen A, Braverman IM. Ultrastructure of the human dermal microcirculation: The horizontal plexus of the papillary dermis. J Invest Dermatol. 1976; 66:131–142. [PubMed: 1249441]
48. Petzelbauer P, Pober J, Keh A, Braverman I. Inducibility and expression of microvascular endothelial adhesion molecules in lesional, perilesional, and uninvolved skin of psoriatic patients. J Invest Dermatol. 1994; 103:300–305. [PubMed: 7521374]
49. Braverman IM, Yen A. Ultrastructure of the human dermal microcirculation. Ii. The capillary loops of the dermal papillae. J Invest Dermatol. 1977; 68:44–52. [PubMed: 830769]
50. Braverman IM. Ultrastructure and organization of the cutaneous microvasculature in normal and pathologic states. J Invest Dermatol. 1989; 93:2S–9S. [PubMed: 2666519]
51. Fina L, Molgaard HV, Robertson D, Bradley NJ, Monaghan P, Delia D, Sutherland DR, Baker MA, Greaves MF. Expression of the CD34 gene in vascular endothelial cells. Blood. 1990; 75:2417–2426. [PubMed: 1693532]
52. Zimmerman M, McGeachie J. Quantitation of the relationship between aortic endothelial intercellular cleft morphology and permeability to albumin. Atherosclerosis. 1986; 59:277–282. [PubMed: 3964349]
53. Iden S, Misselwitz S, Peddibhotla SS, Tuncay H, Rehder D, Gerke V, Robenek H, Suzuki A, Ebnet K. aPKC phosphorylates JAM-A at ser285 to promote cell contact maturation and tight junction formation. J Cell Biol. 2012; 196:623–639. [PubMed: 22371556]
54. Mertens AE, Rygiel TP, Olivo C, van der Kammen R, Collard JG. The Rac activator Tiam1 controls tight junction biogenesis in keratinocytes through binding to and activation of the Par polarity complex. J Cell Biol. 2005; 170:1029–1037. [PubMed: 16186252]
55. Koto T, Takubo K, Ishida S, Shinoda H, Inoue M, Tsubota K, Okada Y, Ikeda E. Hypoxia disrupts the barrier function of neural blood vessels through changes in the expression of claudin-5 in endothelial cells. Am J Pathol. 2007; 170:1389–1397. [PubMed: 17392177]
56. Stiemke MM, McCartney MD, Cantu-Crouch D, Edelhauser HF. Maturation of the corneal endothelial tight junction. Invest Ophthalmol Vis Sci. 1991; 32:2757–2765. [PubMed: 1894473]

57. Bazzoni G, Dejana E. Endothelial cell-to-cell junctions: Molecular organization and role in vascular homeostasis. Physiological Reviews. 2004; 84:869–901. [PubMed: 15269339]
58. Mertens AE, Pegtel DM, Collard JG. Tiam1 takes part in cell polarity. Trends Cell Biol. 2006; 16:308–316. [PubMed: 16650994]
59. Yuan L, Le Bras A, Sacharidou A, Itagaki K, Zhan Y, Kondo M, Carman CV, Davis GE, Aird WC, Oettgen P. ETS-related gene (ERG) controls endothelial cell permeability via transcriptional regulation of the claudin 5 (cldn5) gene. J Biol Chem. 2012; 287:6582–6591. [PubMed: 22235125]
60. Fontijn RD, Rohlena J, van Marle J, Pannekoek H, Horrevoets AJ. Limited contribution of claudin-5-dependent tight junction strands to endothelial barrier function. Eur J Cell Biol. 2006; 85:1131–1144. [PubMed: 16959372]
61. Ades EW, Candal FJ, Swerlick RA, George VG, Summers S, Bosse DC, Lawley TJ. HMEC-1: Establishment of an immortalized human microvascular endothelial cell line. J Invest Dermatol. 1992; 99:683–690. [PubMed: 1361507]
62. Aird WC. Phenotypic heterogeneity of the endothelium:I. Structure, function, and mechanisms. Circ Res. 2007; 100:158–173. [PubMed: 17272818]
63. Hordijk PL, Anthony E, Mul FP, Rientsma R, Oomen LC, Roos D. Vascular-endothelial-cadherin modulates endothelial monolayer permeability. J Cell Sci. 1999; 112(Pt 12):1915–1923. [PubMed: 10341210]
64. Grab DJ, Nikolskaia O, Kim YV, Lonsdale-Eccles JD, Ito S, Hara T, Fukuma T, Nyarko E, Kim KJ, Stins MF, Delannoy MJ, Rodgers J, Kim KS. African trypanosome interactions with an in vitro model of the human blood-brain barrier. J Parasitol. 2004; 90:970–979. [PubMed: 15562595]
65. Vu K, Weksler B, Romero I, Couraud PO, Gelli A. Immortalized human brain endothelial cell line HCMEC/D3 as a model of the blood-brain barrier facilitates in vitro studies of central nervous system infection by cryptococcus neoformans. Eukaryot Cell. 2009; 8:1803–1807. [PubMed: 19767445]
66. Nakagawa S, Deli MA, Nakao S, Honda M, Hayashi K, Nakaoke R, Kataoka Y, Niwa M. Pericytes from brain microvessels strengthen the barrier integrity in primary cultures of rat brain endothelial cells. Cell Mol Neurobiol. 2007; 27:687–694. [PubMed: 17823866]
67. Shimizu F, Sano Y, Saito K, Abe MA, Maeda T, Haruki H, Kanda T. Pericyte-derived glial cell line-derived neurotrophic factor increase the expression of claudin-5 in the blood-brain barrier and the blood-nerve barrier. Neurochem Res. 2012; 37:401–409. [PubMed: 22002662]
68. Baluk P, Fuxe J, Hashizume H, Romano T, Lashnits E, Butz S, Vestweber D, Corada M, Molendini C, Dejana E, McDonald DM. Functionally specialized junctions between endothelial cells of lymphatic vessels. J Exp Med. 2007; 204:2349–2362. [PubMed: 17846148]
69. Pfeiffer F, Kumar V, Butz S, Vestweber D, Imhof BA, Stein JV, Engelhardt B. Distinct molecular composition of blood and lymphatic vascular endothelial cell junctions establishes specific functional barriers within the peripheral lymph node. Eur J Immunol. 2008; 38:2142–2155. [PubMed: 18629939]
70. Kriehuber E, Breiteneder-Geleff S, Groeger M, Soleiman A, Schoppmann SF, Stingl G, Kerjaschki D, Maurer D. Isolation and characterization of dermal lymphatic and blood endothelial cells reveal stable and functionally specialized cell lineages. J Exp Med. 2001; 194:797–808. [PubMed: 11560995]

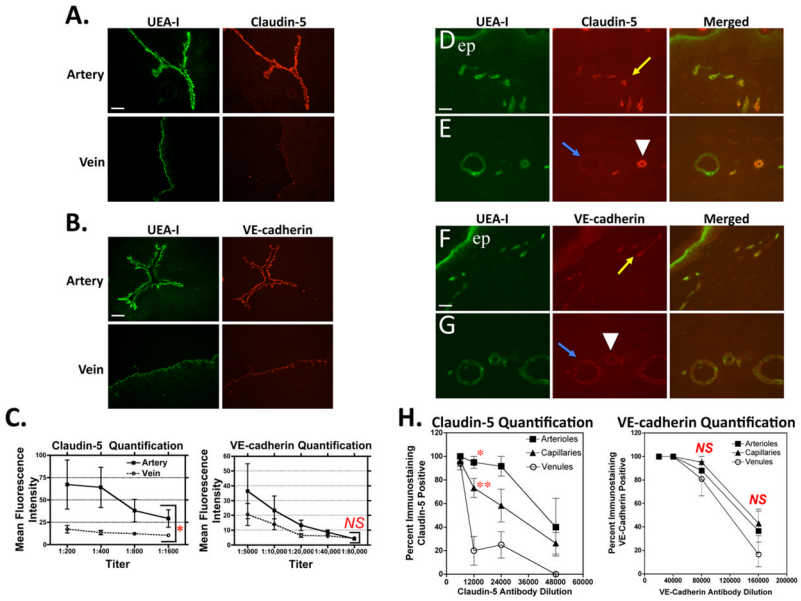

Figure 1.

Claudin-5 and VE-cadherin expression *in situ*. Epifluorescence micrographs of human umbilical artery and vein ECs identified by staining with FITC-Ulex Europeus Agglutinin I (UEA-I) and assessed for expression levels of **(A)** claudin-5 and **(B)** VE-cadherin by immunostaining with rabbit anti-claudin-5 or rabbit anti-VE-cadherin primary antibodies at 1:400 and 1:5000 dilutions, respectively. Scale bars = 100 μm. **(C)** Quantitation of fluorescence intensities showing mean fluorescence intensity +/− SD (y-axis) vs. antibody titer (x-axis). Differences comparing arteries to veins are statistically significant at for anti-claudin-5 (*P = 0.02) and not statistically significant for anti-VE-cadherin (P = 0.71) by paired t-test. Representative of two (claudin-5) and three (VE-cadherin) umbilical cord specimens analyzed with similar results. Fluorescence micrographs of human dermal microvascular segments identified by UEA-I staining and assessed for expression levels of **(D and E)** claudin-5 and **(F and G)** VE-cadherin by immunostaining at primary antibody dilutions of 1:3,000 and 1:20,000, respectively. Scale bars = 25μm. **(H)** Fluorescence micrographs scored as positive or negative are shown as the mean of the percent positive +/− SEM at each antibody dilution. Differences are statistically significant at a 1:12,000 dilution of anti-claudin-5 (*P < 0.001 for arterioles vs. venules and **P< 0.01 for capillaries vs. venules by a one-way ANOVA comparison, Bonferroni post-test correction) but not at any antibody dilution for VE-cadherin. *Yellow arrows, dermal capillary; blue arrows, venule; arrowheads, arteriole*; “ep”, epidermis. Representative of four skin specimens analyzed with similar results.

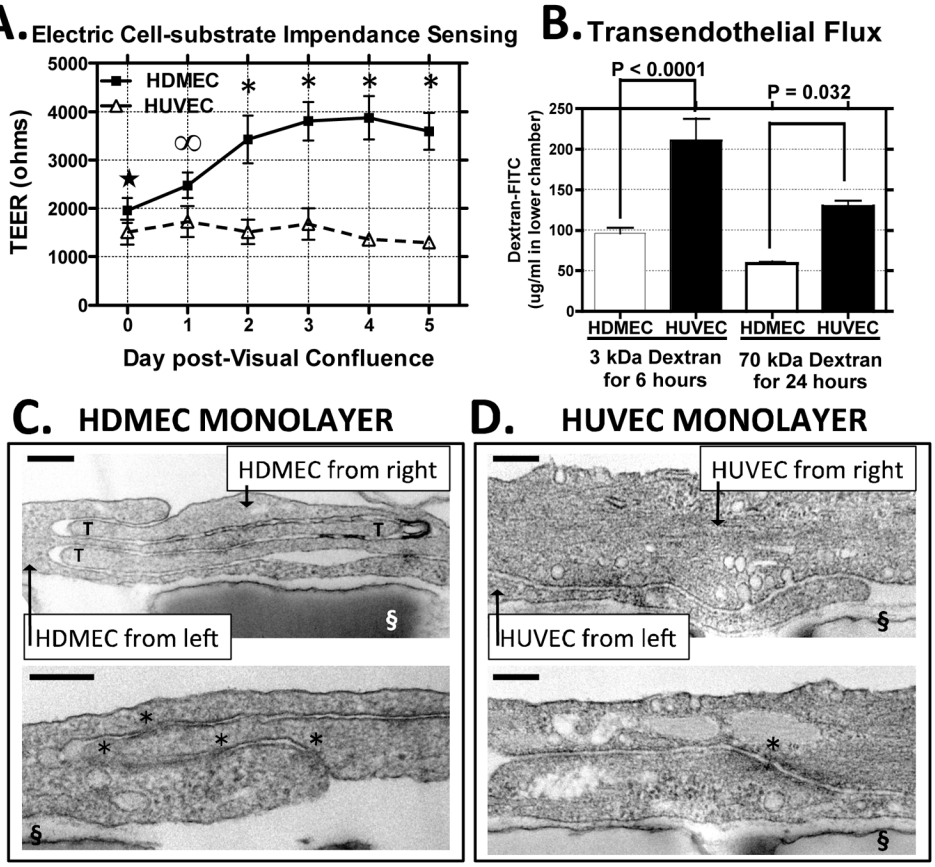

Figure 2.

Paracellular barriers and junctional ultrastructure of HDMEC and HUVEC monolayers. **(A)** TEERs of HDMEC and HUVEC monolayers measured by ECIS presented as mean +/−SEM as a function of day post-visual confluence. Statistical significance was assessed by two-way ANOVA with Bonferroni post-test correction, *, $P < 0.0001$; ∞, $P< 0.001$;☆, $P < 0.05$. Pooled data from eight independent experiments with eight different HDMEC and seven different HUVEC isolates. **(B)** Permeability of HDMEC and HUVEC monolayers measured by transendothelial flux of FITC-dextrans of 3 kD (n = 6, 6) and of 70 kD (n = 5, 5) over 6 h and 24 h, respectively at 37°C. Differences in the level of flux between HDMEC and HUVEC monolayers is presented as means +/−SEM; Statistical significance was assessed by an unpaired two-tailed t-test with P values as indicated. Representative of two experiments with similar results. **(C, D)** Transmission electron micrographs of peri-junctional regions of overlap for adjacent (C) HDMECs and (D) HUVECs from day 3 post-visual confluence. Upper panels: Interdigitating tongue-in groove structures are indicated by "T" symbols. Lower panels: Microscope fields of the same specimens depicting "kissing points" as indicated by asterisks. The transwell substrate surface perforated by 0.4 μm pores is labeled "§". Scale bars = 200 nm. Representative of transmission EM analyses on three different HDMEC cultures and on two different HUVEC cultures.

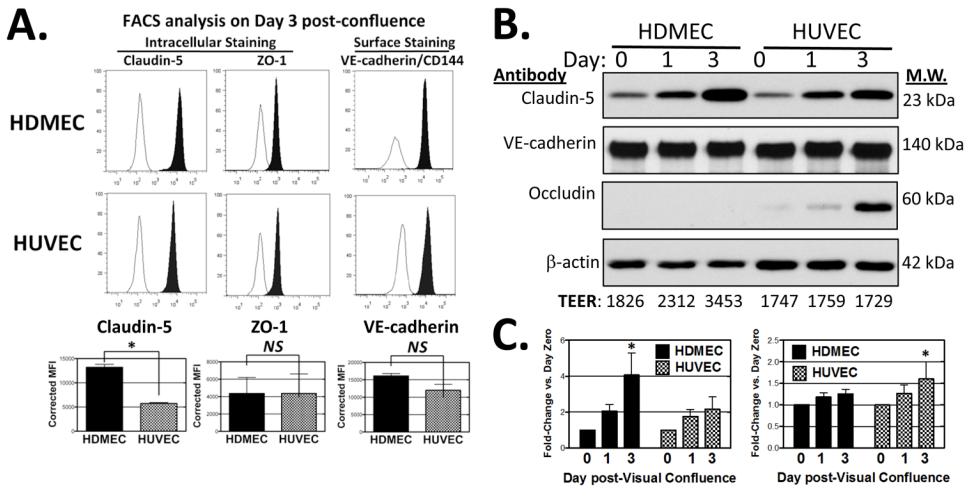

Figure 3.

Junctional protein expression in HDMECs and HUVECs. **(A)** Histograms of FACS analyses comparing HDMEC and HUVEC from cultures at day 3 post-visual confluence immunostained with mouse anti-human VE-cadherin mAb (clone 16B1 directed at an extracellular epitope) and with mouse anti-human claudin-5 and anti-ZO-1 (on permeabilized cells). Filled histograms depict specific antibody staining and open histograms are that of isotype control. *Bottom:* Quantitative analysis from 3 independent experiments showing mean fluorescence intensities corrected for isotype-matched controls. Statistical significance was assessed by two-tailed unpaired t-test *P = 0.0003 for claudin-5 expression; Not significant (N.S.) for ZO-1 or VE-cadherin. **(B)** Representative immunoblot of selected junctional proteins from replicate HDMEC and HUVEC monolayers harvested on day 0, 1 and 3 post-visual confluence. *Numbers below blot*: TEER values recorded on day 0, 1 and 3 of replicate EC cultures plated in parallel to those analyzed by immunoblotting. **(C)** Densitometric analyses comparing HDMEC and HUVEC expression of claudin-5 and VE-cadherin normalized to that of β-actin pooling data from several independent experiments. Statistical significance relative to expression on Day 0 post-confluence was assessed by two-way ANOVA with Bonferroni post-test correction; *P < 0.5 for claudin-5 in HDMEC (n=5, 5), *P < 0.05 for VE-cadherin in HUVEC (n = 6, 6).

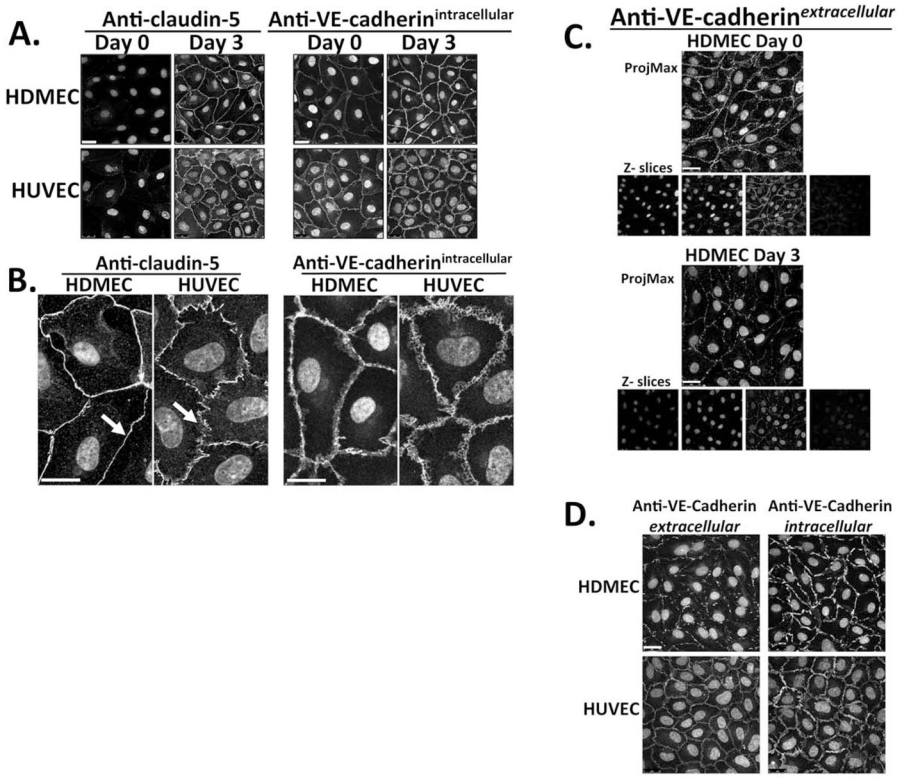

Figure 4.

Confocal immunofluorescence micrographs of HDMEC and HUVEC junctional proteins. Maximum intensity projections showing claudin-5 and VE-cadherin expression in permeabilized HDMEC and HUVEC **(A)** on days 0 and 3 post-visual confluence and **(B)** on day 3 at lower and higher magnification, respectively. Nuclei stained with DAPI. One of three independent experiments with similar results. Scale bar in (A) = 25 μm, in (B) = 100 μm. In (B), arrows highlight fine continuous patterning of junctional claudin-5 in HDMEC and the sawtooth discontinuous claudin-5 patterning in HUVEC. **(C)** Immunostaining of HDMEC with mouse mAb BV6 of an extracellular VE-cadherin epitope on HDMEC (without permeabilization) contrasting day 0 and day 3 post-visual confluence. Scale bar = 25 μm. *Below:* 0.8 μm optical Z-sections from each projection. **(D)** Immunostaining of HDMEC (top) and HUVEC (bottom) on day 3 post- visual confluence for a VE-cadherin extracellular epitope (antibody BV6, no cell permeabilization, left panels) and for an intracellular epitope (goat anti-VE-cadherin, in permeabilized cells, right panels). Representative of four independent experiments with similar results. Scale bar = 25 μm.

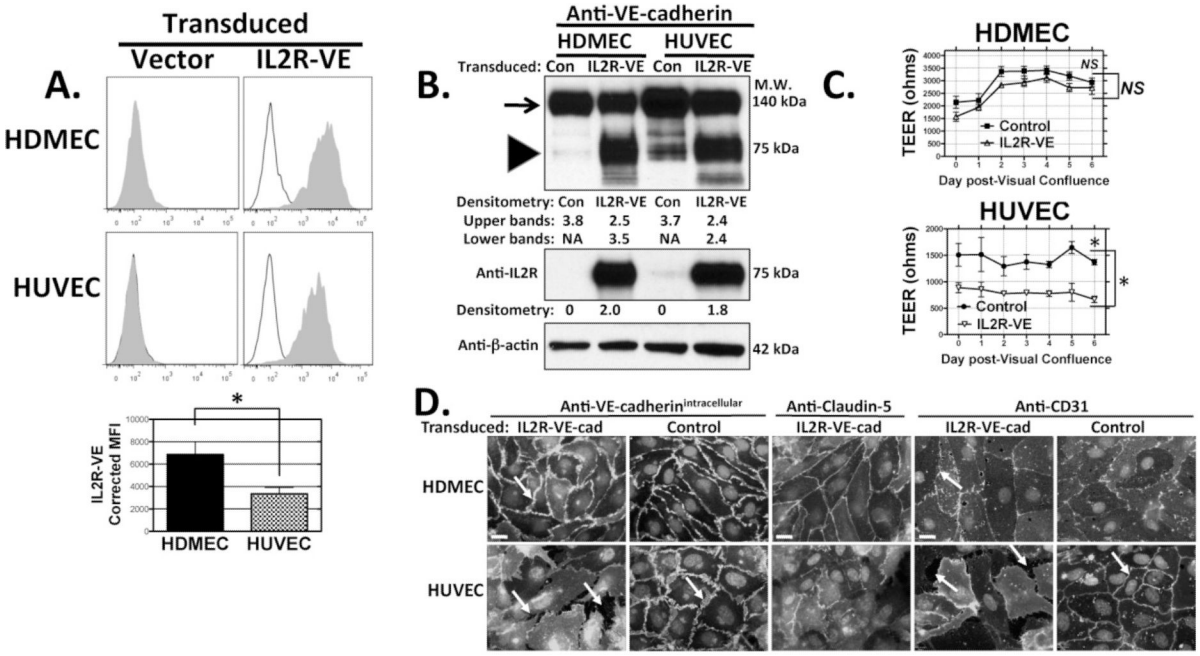

Figure 5.

Effects of dominant negative VE-cadherin protein overexpression. **(A)** FACS analyses of IL-2Rα immunostaining of HDMECs and HUVECs transduced with plasmid LZRS empty vector control (left) or with the otherwise identical retroviral vector containing an IL2R-VE insert (right). The IL2R-VE transductants were selected previously by positive FACS sorting with anti-IL- 2Rα. Specific staining (filled histograms) with APC-conjugated anti-IL2Rα is compared to staining with isotype control (empty histograms). *Bottom:* Mean fluorescence intensity of IL2R- VE overexpression corrected for isotype control from three independent experiments. * P = 0.04 by unpaired two-tailed t-test. **(B)** Immunoblotting of cell lysates of the same transduced cell cultures shown in panel A. *Top panel:* Protein lysates from empty LZRS vector control- and IL2R-VE-cadherin-transduced HDMECs (lanes 1 and 2) or HUVECs (lanes 3 and 4) analyzed with rabbit anti-VE-cadherin. *Arrow*: band representing endogenous VE-cadherin; *Arrowhead:* IL2R-VE-cadherin fusion protein. The same protein lysates were analyzed by immunoblotting with goat- anti-IL2Rα (*middle panel)* or anti-β-actin *(bottom panel)*. Numbers indicate densitometric analyses of the immunoblot data normalized to expression of β-actin. **(C)** TEER development in HDMECs and HUVECs transduced with dominant negative IL2R-VE-cadherin. Over a six day time course starting at post-confluence, TEER levels did not differ between control and IL2R-VE transduced HDMECs (NS, not significant by one way ANOVA with a Bonferonni correction and not significant by two-tailed t-test on day 6) but were consistently different between control and IL2R-VE-transduced HUVEC (*P < 0.05 by one way ANOVA with a Bonferonni correction and P = 0.0005 by two-tailed t-test on day 6). Mean TEER values were analyzed from four independent experiments. **(D)** Immunofluorescence staining of FACSorted EC for VE-cadherin (with goat anti-VE-cadherin to an intracellular epitope, left), and for claudin-5 (middle) on permeabilized cells and for CD31/PECAM-1 (right, but on intact cells) comparing empty vector control and IL2R-VE transduced HDMECs and HUVECs at day 3 post-visual confluence. Arrows show where IL2R-VE-transduced HUVECs but not HDMECs form gaps. Scale bar = 15 μm. The experiments shown in Figure 5 are representative of three sets of transduced EC lines analyzed with similar results.

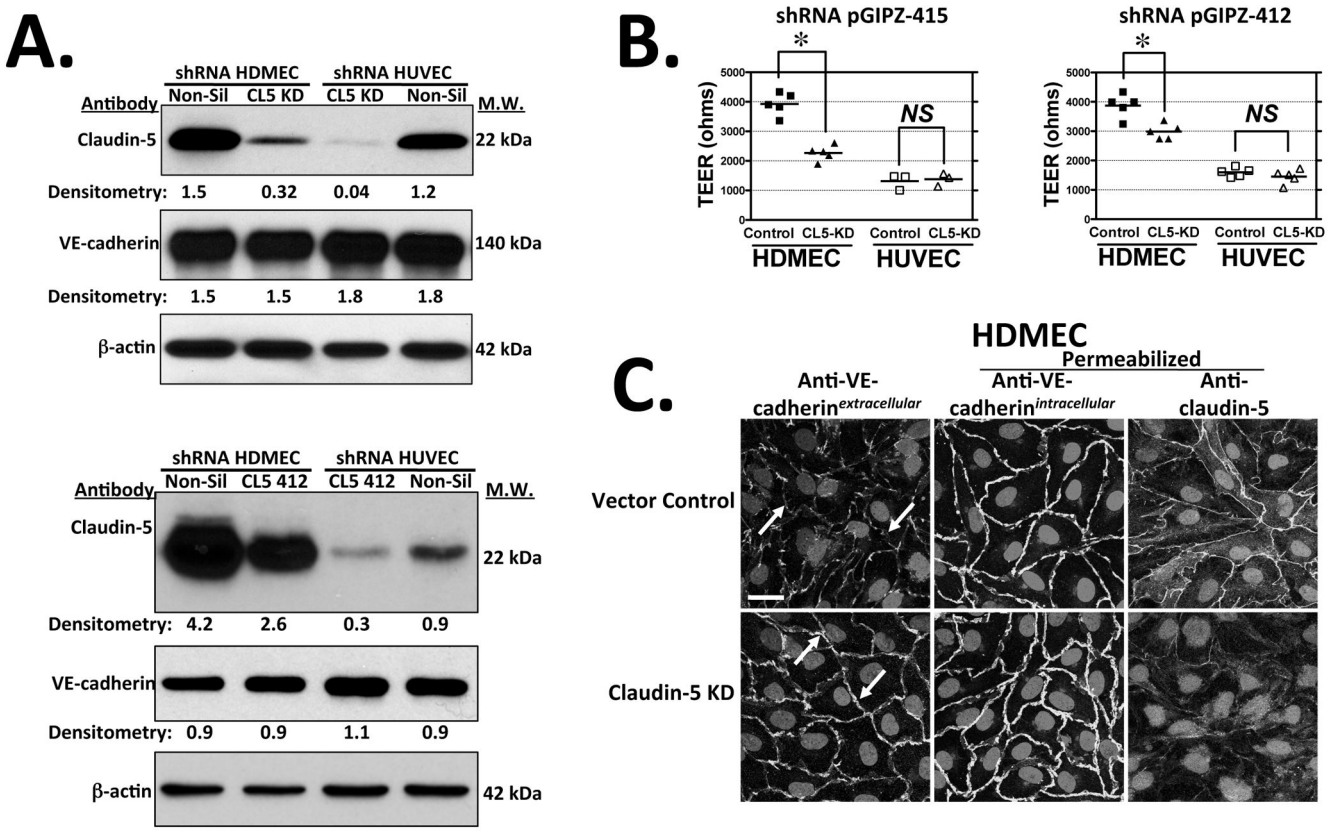

Figure 6.

ShRNA knockdown of claudin-5 in HDMECs and HUVECs. **(A)** Top: Immunoblot analysis of claudin-5 expression in HDMECs (left) and HUVECs (right) transduced with non-silencing lentivirus vector control (Non-Sil) or with claudin-5 shRNA clone V2LHS_171415 (CL5 KD; top panel) or with a second claudin-5 shRNA, clone V2LHS_171412 (bottom panel) at day 4 post-visual confluence. Numbers indicate densitometric analyses of the immunoblot data normalized to expression of β-actin. **(B)** TEER levels in HDMECs or HUVECs stably transduced with shRNA pGIPZ clone V2LHS_171415 (pGIPZ-415) or clone V2LHS_171412 (pGIPZ-412) vs. non-silencing (Non-Sil) shRNA negative control-transduced ECs on day 3 post-confluence. Knockdown of claudin-5 in HDMECs significantly reduced TEER ($p < 0.0001$ and $p < 0.005$ by two-tailed t test for GIPZ-415 and GIPZ412, respectively) whereas no significant TEER differences are observed in HUVECs transduced with either shRNA. TEER values shown are means from multiple experiments with pGIPZ-415 (n = 5, 3) and with pGIPZ-412 (n= 5, 5). **(C)** Confocal fluorescence optical z-sections of vector control (upper panels) vs. claudin-5 knockdown HDMEC (lower panels) monolayers at day 4 post-visual confluence immunostained with mouse mAb BV6 to VE-cadherin extracellular epitopes in non-permeabilized cells (arrows indicate differential antibody accessibility) and goat anti-VE-cadherin antibody to intracellular epitopes or rabbit anti-claudin-5 antibody in permeabilized cells. Scale bar = 15 μm. One of three experiments with similar results.

Table I

Ultrastructural features of day 3 post-visual confluent HDMEC and HUVEC monolayers

EC Type	Tongue-in-groove structures per overlap region +/− SEM	Tight Junctions per overlap region +/− SEM	Maximum TEER in ohms +/− SEM
HDMEC *	1.77 +/− 0.25	4.94 +/− 0.67	3939 +/− 122
HUVEC †	0.29 +/− 0.13	1.53 +/− 0.19	1478 +/− 36
Unpaired two-tailed t-test	Significant: $P < 0.0001$	Significant: $P < 0.0001$	Significant: $P < 0.0001$

* Pooled data from 3 different isolates.

† Pooled from 2 different isolates.